Atomistic investigation of the influence of Hydrogen on dislocation nucleation during nanoindentation in Ni and Pd

Xiao Zhou[a], Bin Ouyang[a], W. A. Curtin[b], Jun Song[a, *]

[a] Department of Mining and Materials Engineering, McGill University, Montreal, QC, Canada

[b] Institute of Mechanical Engineering, Ecole Polytechnic Federale de Lausanne, Switzerland

Abstract

The effects of hydrogen charging on the mechanical response of FCC Ni and Pd under nanoindentation are systematically investigated by molecular dynamics simulations. Simulations consider a random H distribution and time scales prevent any diffusion of H during the simulations. Hydrogen charging is then found to reduce the threshold load for dislocation nucleation, i.e., the *pop-in* load, but only to a limited extent. After *pop-in*, the indentation response is largely independent of the presence of H. Furthermore, the influence of hydrogen charging on the *pop-in* load originates only from the hydrogen-induced swelling of the lattice. That is, H does not directly influence dislocation nucleation, either in terms of facilitating initial slip or interacting with the nascent dislocation(s). These findings suggest that rate-dependent processes, either associated with fluctuating nucleation or H transport, are necessary to interpret experimental observations of hydrogen-influenced reductions in the *pop-in* load.

Keywords: Hydrogen embrittlement; Nanoindentation; Molecular dynamics simulations;

[*] Author to whom correspondence should be addressed. E-Mail: jun.song2@mcgill.ca

1. Introduction

Hydrogen is an impurity often present in structural materials during production and service. The mechanical failure due to the deleterious effect of hydrogen is called hydrogen embrittlement (HE), which is a common problem for various structural metals and alloys [1-6]. It can cause catastrophic failure in load bearing metallic components and poses a serious challenge for material design in industries. Given its significant technological importance and industrial relevance, HE has been extensively studied both theoretically and experimentally. Various models have been proposed in the literature, including H-enhanced decohesion (HEDE) [7-12], H-enhanced local plasticity (HELP) [13-15], hydride formation and cleavage [16-18], and recently a model [19, 20] based on H-induced local "*ductile-to-brittle*" transition at the crack. All of these models have merits, but none fully captures the scope of Hydrogen-induced effects on the mechanical properties of metals. The precise HE mechanism(s) and relevant length and time scales, remain a topic of vigorous discussion [21].

In parallel, enormous efforts have been placed on developing accurate and efficient experimental methods in order to better capture and visualize the material behaviors during HE and other effects of Hydrogen on plastic flow. Besides the conventional HE index approach [22, 23] to examine HE at macroscopic scale, the local examination at the crack tip [13, 24-26] and the *in-situ* transmission electron microscope (TEM) examination of dislocations [27-30] are often used as means to probe the H effects at microscopic level. Another experimental approach to investigate the effects of Hydrogen on plasticity at small scales is instrumented nanoindentation (NI) [31, 32]. NI has the capacity to resolve dislocation nucleation in extremely small volumes [33-39], and has been extended by Barnoush and Vehoff [40] to *in-situ* electrochemical nanoindentation (ECNI).

In the NI/ECNI experiments, the material modulus and *pop-in* load are measured at fixed surface electrochemical potential. The presence of H is often found to reduce the *pop-in* load [40], although different effects are observed in different materials. The reduction has been attributed to reductions in dislocation line tension and/or shear modulus in the presence of H, which facilitate homogeneous dislocation nucleation (HDN). However the *pop-in* event during nanoindentation is a collective behavior corresponding to simultaneous burst of multiple dislocations, and is not directly HDN. Mechanistically, the reduction of line tension is envisioned due to segregation of H to dislocations, which would presumably not occur for HDN since no stable dislocation exists prior to the nucleation event. Thus, the origins of the reduction of *pop-in* load due to H remain unclear.

The role of various "side effects" associated with H charging, such as H-induced lattice swelling and vacancy crowding [41-43], on effecting the *pop-in* load have not been directly addressed in experiments. In a recent study [44], atomistic simulations studied how other pre-existing defects (vacancies and stacking fault tetrahedra) influence the nanoindentation response of single-crystal copper and showed that those structural defects can cause significant reductions in the *pop-in* load at low temperature. Thus, further investigation is required to elucidate the exact influence of H on nanoindentation response including its role in stabilizing other defects and, in general, understanding the onset of dislocation at more refined length and time scales.

In this paper, we employ molecular dynamics (MD) simulations to probe various direct and indirect effects of H on nanoindentation response at the atomic scale. Specifically, the force-displacement responses of Ni and Pd single crystals of different crystal orientations deformed under a rigid indenter are examined with and without interstitial H. We find very limited effects of H on the *pop-in* load, with the effects entirely explained by lattice dilation introduced by H

such that there is no direct H effect on *pop-in*. The response after *pop-in* does not show any distinct role of H. We then discuss the implications of our results for mechanisms of observed effects of H on nanoindentation, pointing toward future directions for research in this area.

2. Computational Methodology

We utilized large-scale MD simulations to examine the deformation behaviors of two model M-H systems (M=Ni, Pd) during nanoindentation. For each M-H system, two initial rectangular simulation cells, each consisting of a FCC M single crystal, with one oriented as $X = [\bar{1}10]$, $Y = [001]$ and $Z = [110]$, and the other oriented as $X = [\bar{1}10]$, $Y = [\bar{1}\bar{1}2]$ and $Z = [111]$ are created, where Z is the surface that will be indented. Sample dimensions are (L_x, L_y, L_z) being (28.0nm, 28.3nm, 14.5nm) and (28.0nm, 27.7nm, 14.6nm) for Ni-H, and (22.0nm, 20.8nm, 16.0nm) and (22.0nm, 20.9nm, 16.2nm) for Pd-H. Starting from each initial atomic configuration, several systems are created for simulations, as described below. In all case, the simulation cell is periodic along the *X* and *Y* directions, while free boundary condition is applied along *Z* direction, i.e., both top and bottom surfaces along *Z* are traction-free. The center of mass of the material is held fixed during the indentation to prevent rigid translational motions. Below, the *Z* direction is used to represent the crystal orientation.

With the above general information, we consider two types of samples. The first set of samples are metals charged with Hydrogen. H atoms are introduced by randomly inserting them into the octahedral sites in the M lattice to create an M-H system at a desired H concentration. The resultant M-H system is then relaxed within the NPT ensemble (*i.e.*, T = 300K, $\sigma_{xx} = \sigma_{yy} = 0$) for 1.5 ns. Three M-H systems having 0%, 2% and 4% atomic H per M atom are studied for each crystal orientation, and are referred to as pure M, $MH_{0.02}$ and $MH_{0.04}$ systems, respectively.

These H concentrations are expected to be comparable to those prevailing in the experiments of Barnoush and Vehoff [40], estimated to be ~3% [45]. For each H concentration, four different random H distributions are generated. The second set of samples are Hydrogen-free systems subjected to an in-plane equi-biaxial strain prior to indentation. The initial simulation cell is first relaxed within the NPT ensemble (*i.e.*, T = 300K, $\sigma_{xx} = \sigma_{yy} = 0$) for 1.5ns. The simulation cell is then uniformly stretched/compressed along both X and Y directions to lattice strains ε from -0.9% to 1.4%.

All systems are then further relaxed in the NVT ensemble [46, 47] (*i.e.*, T = 300K) for 0.5ns to reach an equilibrium state. Nanoindentation is then conducted by moving a virtual spherical indenter with tip radius of 10 nm along the Z direction towards the material at a constant velocity of 10 m/s [48] until the desired indentation depth is reached. The indenter is modeled as a *rigid* indenter using a strongly repulsive potential by Kelchner et al. [49]. During indentation, the linear momentum of the material along Z direction is reset to zero at every timestep and the force on the indenter and evolution of material microstructure is monitored. The lattice defects generated during deformation are quantitatively visualized using the common neighbor analysis (CNA) [50] and the deformation index (DI) method by Wen et al. [51, 52]. At finite temperature, the nucleation process is thermally activated, and so conduct four simulations with different initial temperature seeds for each configuration to estimate the average nucleation force for the given indentation rate and temperature.

For later reference, we also compute the elastic response of the M-H materials here. The shear modulus $\mu_{\mathrm{M(H)M}}$ associated with (111) shearing [53] as a function of H concentration c_{H} for Ni-H and Pd-H systems are shown in Figure 1. In both cases, $\mu_{\mathrm{M(H)M}}$ decreases

approximately linearly with increasing H concentration. The decrease is not large, however: at c_H = 4%, the modulus decreases by ~4.5% for Ni and by ~8.5% for Pd.

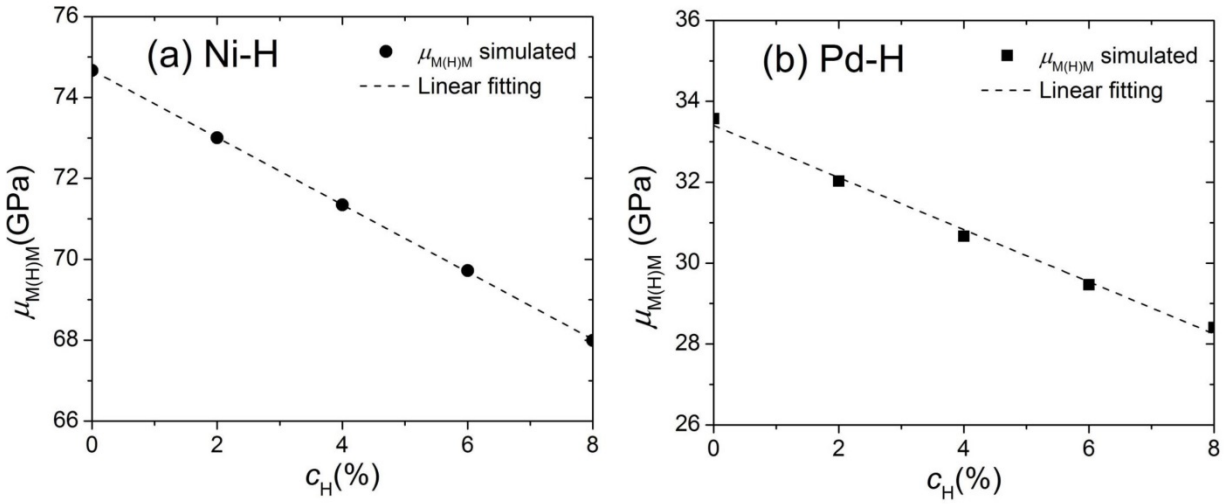

Figure 1: Shear modulus $\mu_{M(H)M}$ associated with (111) shearing ([51]) versus atomic H concentration c_H for (a) Ni-H and (b) Pd-H systems.

The MD simulations are performed using the LAMMPS code [54]. The system evolves using a Nosé–Hoover thermostat [47, 55] and velocity-Verlet algorithm [56] with integration time steps of 1 femtosecond (fs). The interatomic interactions in the Ni-H system are described using an embedded-atom-method (EAM) potential [57, 58] developed by Angelo et al. while the EAM potential developed by Zhou et al. is adopted for the Pd-H system in this study [59].

3. Results

3.1. Indentation of Ni-H and Pd-H

The load on the indenter F_z versus the indentation depth δ is shown in Figure 2 for the pure Ni, $NiH_{0.02}$ and $NiH_{0.04}$ systems, for both crystal orientations. All F_z vs. δ curves exhibit a

range of load drops associated with dislocation nucleation, annihilation and exit from the free surface, for which the corresponding dislocation dynamics/reactions are well documented [60-62]. In particular, the first load drop in F_z vs. δ corresponds to the onset of plasticity, *i.e.*, the first dislocation nucleation event (HDN). We denote the point of the maximum force and displacement just prior to the first load drop as F_z^c and δ^c, which are effectively the *pop-in* load and the threshold indentation depth corresponding to the onset of plasticity in our computational indentation experiments. The insets to Figure 2 show the response around F_z^c and δ^c versus H concentration more clearly. In the elastic loading phase, the F_z vs. δ curves overlap, but the *pop-in* load, and thus the threshold indentation depth, decreases with increasing H concentration. After the first load drop, Figure 2 shows that the response at larger indentation depths is approximately independent of H concentration; that is, no distinct trend can be found in the magnitude or sequence of subsequent load drops. These results suggests that H facilitates the onset of plasticity (HDN), in agreement with the previous simulations by Wen et al. [52], but does not cause any subsequent softening effect at higher displacements as claimed by Wen et al. We return below to the origin of the apparent H reduction of the *pop-in* load below.

The indentation responses for the pure Pd, $PdH_{0.02}$ and $PdH_{0.04}$ systems are shown in Figure 3. Aside from an overall difference in magnitude of the loads at which plastic flow occurs, the general characteristics of the indentation behaviors of Pd and Pd-H systems are similar to the Ni and Ni-H systems. Therefore, the general effect of H among the two materials is solely to reduce the *pop-in* load with increasing H concentration.

The decrease in the *pop-in* load is also much larger than the reduction in shear modulus $\mu_{M(H)M}$ (see Figure 1). Dislocation nucleation is expected to scale with shear modulus, so that

the observed H influence on the *pop-in* load is not simply due to a change in elastic response of the material.

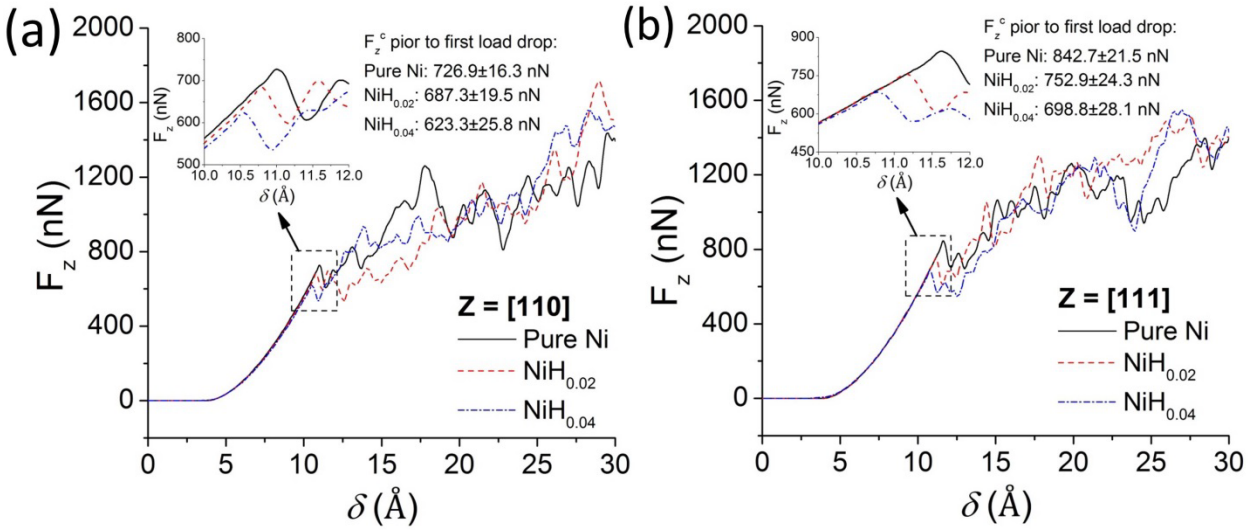

Figure 2 (Color online): the load on indenter (F_z) versus indentation depth (δ) curves for the pure Ni (solid line), $NiH_{0.02}$ (dash line) and $NiH_{0.04}$ (dash dot line) systems with indentation direction (a) Z = [110] and (b) Z = [111]. The inserted figures show the close-up views of the curves around the point where the first load drop occurs.

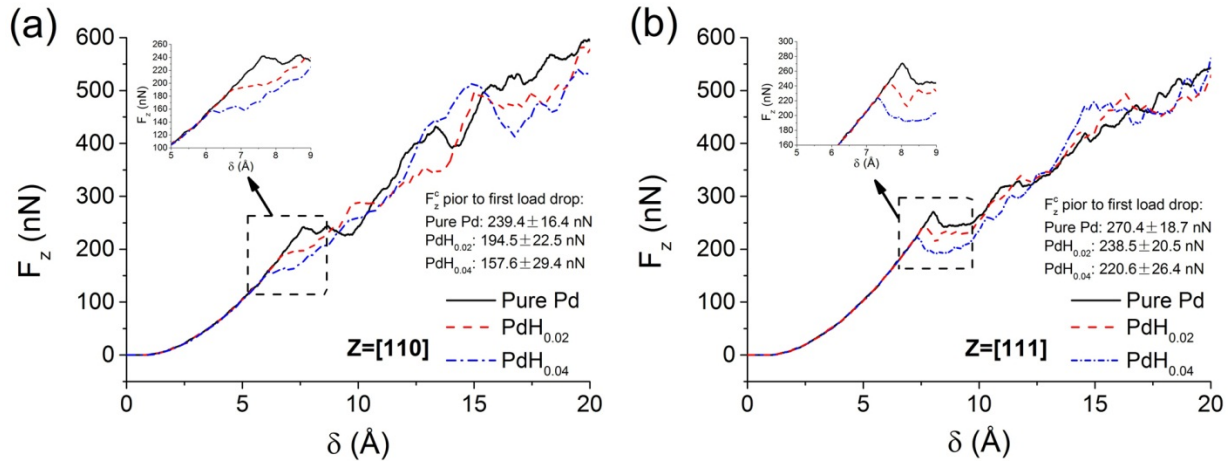

Figure 3 (Color online): the load on indenter (F_z) versus indentation depth (δ) curves for the pure Pd (solid line), $PdH_{0.02}$ (dash line) and $PdH_{0.04}$ (dash dot line) systems with indentation direction (a) Z = [110] and (b) Z = [111]. The inserted figures show the close-up views of the curves around the point where the first load drop occurs.

3.2. Indentation of Pre-strained Ni and Pd

One consequence of H charging is an induced swelling of the lattice relative to the pure metal system. For H in octahedral sites of the fcc lattice, the induced swelling is nearly hydrostatic, associated with the misfit volume Ω_H for H in the host lattice. For a stress-free sample of initial volume V_0 and lattice constant a_0, the volume after charging to atomic concentration c_H is $V_0\left(1+\frac{4c_H\Omega_H}{a_0^3}\right)$. The associated hydrostatic misfit strain tensor is diagonal with components $\varepsilon_H = dV/V_0$, where dV is the volume change, so that $\varepsilon_H = \left(1+\frac{4c_H\Omega_H}{a_0^3}\right)^{1/3} - 1$.

For the Ni-H system, the simulation of a single H in a large Ni lattice yields, for the current interatomic potential, $\Omega_H = 0.075a_0^3$ [58]. The predicted misfit strains are $\varepsilon_H = 0.20\%$ and 0.39% for c_H = 2% and 4%, respectively. The measured volume expansions in the simulations cells studied here correspond to ε_H = 0.18% and 0.37% for the $NiH_{0.02}$ and $NiH_{0.04}$. The volume expansion is measured by comparing the relaxed simulation cell of the H-charged system (along *x* and *y* directions), obtained after the NPT relaxation (see Section 2 for details) to that of the H-free system. Similarly, in Pd, the simulation of a single H in a large Pd lattice yields, for the current interatomic potential, $\Omega_H = 0.085a_0^3$. The predicted values of ε_H are then 0.23% and 0.45% for $PdH_{0.02}$ and $PdH_{0.04}$, respectively, which again agree very well with the values measured in the simulation cells used for indentation, which show $\varepsilon_H = 0.21\%$ and 0.49%, respectively. The good agreement in both Ni and Pd shows that the volume expansion is well-understood within basic theory, and that there are no unusual H-H interactions, at low c_H, that might induce additional distortions.

As a consequence of the H-induced swelling, the Ni and Pd lattices are strained relative to the pure material, even in the absence of any applied boundary stresses in the simulations. We speculated that the lattice strains alone may change the *pop-in* load because the *pop-in* load can be interpreted as a measure of the point of absolute instability of the crystal lattice, which in turn is sensitive to the precise lattice constants and to the non-linear response of the crystal at large deformations [63]. To investigate the effects of lattice strain on nanoindentation behavior, entirely separated from any direct effects of H, we measured F_z vs. δ for pre-strained (in plane biaxial strain) Ni systems. The results are shown in Figures 4a-b for Ni and in Figures 5a-b for Pd. In all cases, a tensile lattice strain (dilation) reduces the *pop-in* load while a compressive lattice strain increases the *pop-in* load. The effect of pre-strain on the subsequent deformation/hardening behavior shows no systematic trends. Thus, the effect of lattice strains in the absence of H is qualitatively identical to the affects found in H-charged materials. Proceeding more quantitatively, Figures 4c-d and 5c-d show the measured *pop-in* load versus imposed lattice strain for Ni and Pd, respectively. The *pop-in* load is linearly dependent on the initial lattice strain over a wide range, deviating only at large compressive strains for the (111) orientation. Moreover, Figures 4c-d and 5c-d also show the measured *pop-in* loads for the H-charged samples at the lattice strains (expansions relative to the pure metal) induced by the presence of H. The *pop-in* loads for the H-charged specimens are nearly identical to those of the same samples without H but expanded to the same lattice strain.

The results in Figures 4 and 5 show that the behavior of Ni and Pd under indentation is determined by the lattice strain, and that the role of H is simply to induce a stress-free lattice strain (relative to the pure material). The presence of H has no further measurable effects, and hence no direct effects on dislocation nucleation or subsequent multiplication and hardening.

That is, the effects of (immobile) H are indirect, arising only due to dilation of the lattice. We find no evidence of any direct H-enhanced dislocation nucleation or mobility, as claimed by Wen et al. [52]. The present simulations show that (immobile) H in otherwise defect-free materials does not have any direct influence on H-enhanced plasticity (e.g. the HELP mechanism).

Previous work on nucleation of dislocations at a crack tip showed that nucleation was suppressed with increasing H concentration due to the increase in unstable stacking fault energy that controls nucleation [64]. Here, at a few percent H, the change in unstable stacking fault energy is small [64]. Furthermore, for indentation, the point of nucleation is not pre-determined and so nucleation can avoid regions of locally higher H concentration fluctuations underneath the indenter. Thus, suppression of nucleation due to an increased unstable stacking fault energy is not an important factor in the present indentation study.

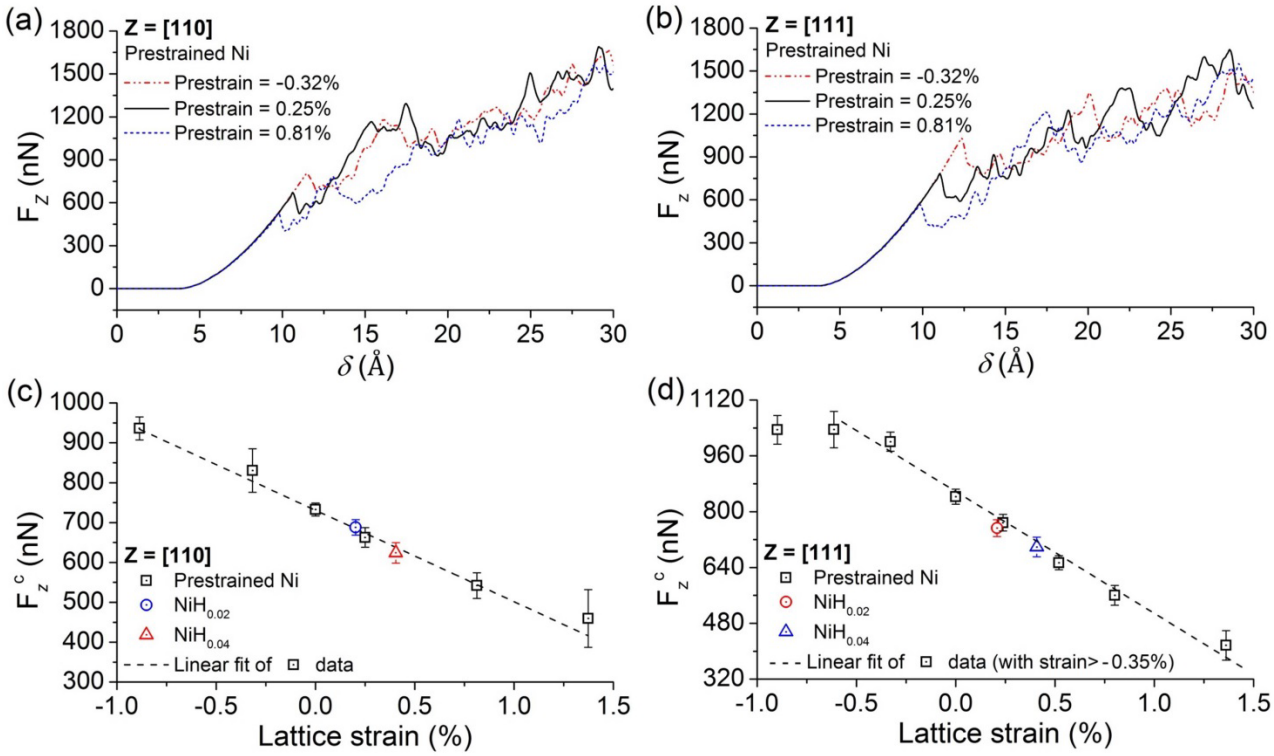

Figure 4 (Color online): The load on indenter (F_z) versus indentation depth (δ) curves for three representative prestrained Ni systems with indentation direction (a) Z = [110] and (b) Z = [111], with (c) and (d)

showing the corresponding load at the first load drop, F_z^c versus lattice strain plot for the prestrained Ni systems (squares) together with the F_z^c versus ε_H data for $NiH_{0.02}$ (circle) and $NiH_{0.04}$ (triangle), where the dashed line is a linear fitting of the square data (in particular for the case with Z=[111], only data with lattice strain > -0.35% are used in the fitting). Note that the values of F_z^c shown in (c) and (d) are average values obtained from the multiple simulations performed for each lattice strain or H concentration (see Section 2), with the associated error bar being the corresponding standard deviation.

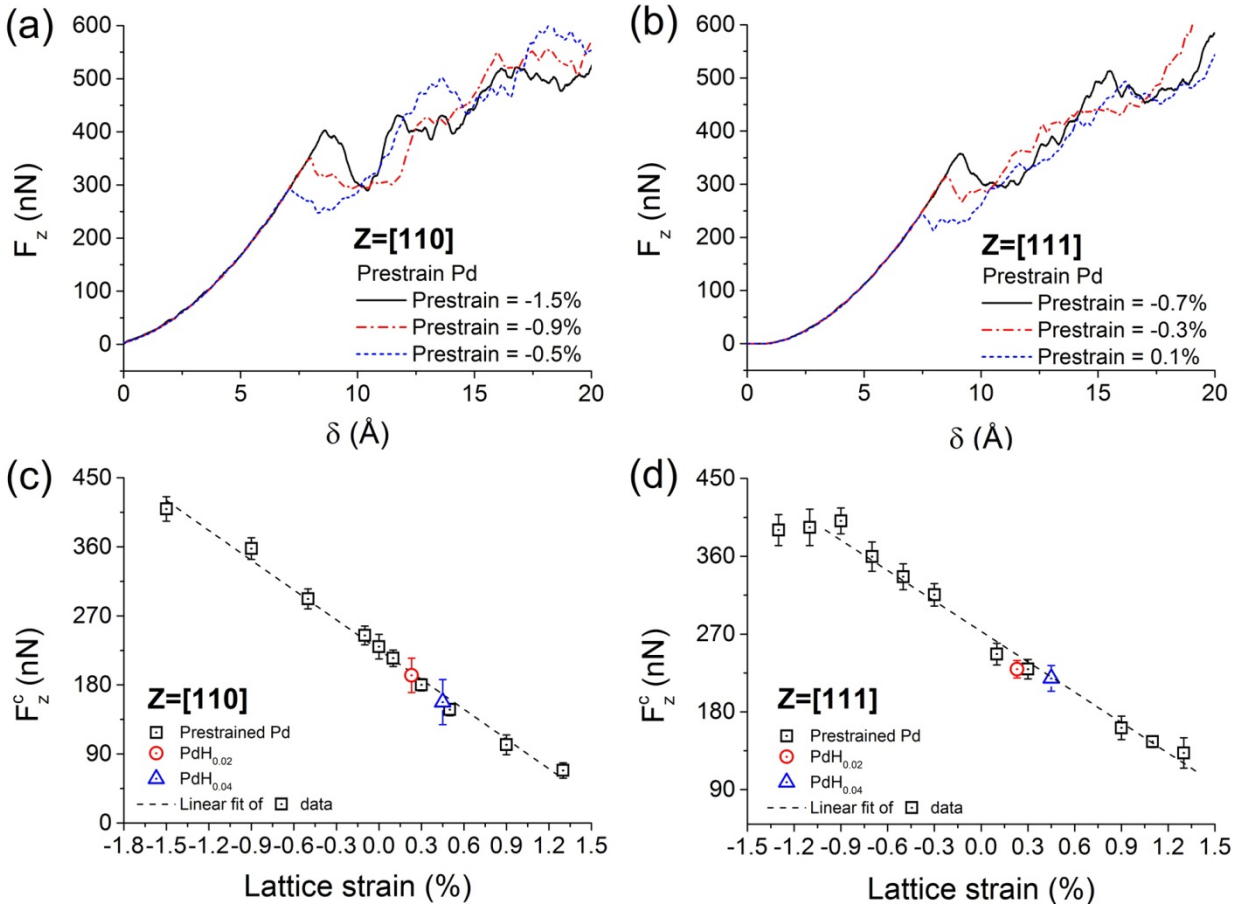

Figure 5 (Color online): The load on indenter (F_z) versus indentation depth (δ) curves for three representative prestrained Pd systems with indentation direction (a) Z = [110] and (b) Z = [111], with (c) and (d) showing the corresponding load at the first load drop, F_z^c versus lattice strain plot for the prestrained Pd systems (squares) together with the F_z^c versus ε_H data for $PdH_{0.02}$ (circle) and $PdH_{0.04}$ (triangle), where the dashed line is a linear fitting of the square data. Note that the values of F_z^c shown in (c) and (d) are average values obtained from the multiple simulations performed for each lattice strain or H concentration (see Section 2), with the associated error bar being the corresponding standard deviation.

4. Discussion

In-situ nanoindentation experiments on homogeneous dislocation nucleation (HDN) in Ni [35-37, 40] show a substantial reduction (e.g., ~51% reduction in the study by Barnoush and Vehoff [40]) in the *pop-in* load following H charging. This is often interpreted as evidence for strong H-dislocation interactions that facilitate the onset of plastic deformation. Our simulations for defect free metals having random H that does not migrate during the duration of the simulation, show that the only effects of H can be attributed to lattice dilation induced by the H. Our results are independent of host metal, for Ni and Pd, and independent of crystal orientation, for [110] and [111] loadings. There is a small reduction in *pop-in* load, but the magnitude is not at all comparable to experiments, and the H concentrations in the simulations and experiments are expected to be comparable [40, 45]. The difference between experiments and simulations indicates that the deformation behavior in experiments involves either rate-dependent processes or processes that involve other defects, or both.

The primary rate-dependent process that could be anticipated is H diffusion during the duration of the experiment. H diffusion in Ni occurs with a migration barrier of ~0.4 eV; this is slow compared to Fe, but yields a mean square diffusion distance at 300K of ~350nm. Thus, it is feasible for H to diffuse in and around the region under stress during nanoindentation. However, if the experiments truly measure HDN in regions of initially dislocation-free material, then there are no initial dislocations toward which H could migrate. At finite temperature, there can be sub-critical dislocation loops that arise as thermal fluctuations, but being fluctuations they do not persist for long periods. Thus, H would have to diffuse sporadically, in response to only the pressure field generated by the fluctuating loops that appear and disappear. Counteracting the possible attraction to such fluctuation loops, however, is the driving force for H diffusion away from regions of high compressive stress. With a positive misfit volume Ω_H, the increase in

chemical potential, relative to bulk H, due to a local compressive pressure of p = 2 GPa (the estimated pressure underneath the indenter at the experimentally-measured *pop-in* load) is $d\mu = p\Omega_H = 0.041$ eV, which drives H away from the region where dislocation nucleation is expected. Experiments further show that when a sample is loaded first and then subsequently charged with H, the *pop-in* load is again reduced relative to the H-free samples. With an increased chemical potential underneath the loaded indenter, the diffusion of H into this region is delayed and the equilibrium concentration is reduced. Therefore, it is difficult to envision that HDN is caused only by mobile H in the bulk lattice.

As mentioned in the Introduction, the presence of defects can reduce the *pop-in* load. If the *pop-in* load is reduced only in the presence of H, then presumably H must stabilize some defects that would not exist in the absence of H. It is well-established that H can bind to vacancies, so that vacancy clusters are stabilized in the presence of H. It is thus possible, in principle, that the presence of H could allow for the formation of stable V_nH_m complexes that would not exist in the H-free material, and that such complexes could serve as nucleation sites for HDN. Preliminary simulations show that vacancy clusters (with or without H) artificially placed underneath the indenter can indeed reduce the *pop-in* load to ~ 2/3 the value in the pure Ni. However, the actual probability of finding such clusters under thermodynamic equilibrium conditions remains quite small. Taking the Ni system as an example, for the interatomic potential here the formation energy of a VH_6 cluster is 0.51 eV (as compared to 1.59 eV for an isolated V), so that the zero-pressure equilibrium concentration of VH_6 at T=300K is estimated to be only ~2×10^{-9}. Thus, one would expect to find one such cluster in every volume of ~ (175 nm)^3 in Ni, which is much larger than the volume probed underneath the nanoindenter. Furthermore, although the misfit volume for a V is negative, the misfit volume for a VH_6

complex is large and positive. Underneath the high pressure of the indenter, the formation enthalpy of the VH_6 complex is thus much higher than at zero pressure, making such complexes thermodynamically even less likely underneath the indenter. Such complexes would have to form prior to the imposition of the indentation load and then, for kinetic reasons, remain stable against dissociation during loading. Since experiments show reduced *pop-in* when the load is imposed prior to charging, this latter scenario does not seem feasible as an explanation of the observed effects.

The above discussion is meant to highlight the fact that the role of H, its presence underneath the indenter, and its role in possibly stabilizing other defects, involves a complicated consideration of kinetic and thermodynamic effects. Any proposed mechanism to explain the experimentally-observed reduction in *pop-in* load upon H charging cannot simply rely on postulated defects or configurations, but must also consider the thermodynamic and kinetic effects that determine the likelihood/probability of occurrence of such postulated defects. This challenge has yet to be undertaken in this field but appears essential for viable physical explanation of the observed phenomena.

Acknowledgements:

The authors acknowledge support of this work by the NSERC Discovery grant (grant # RGPIN 418469-2012) and by the Swiss National Foundation through a grant for the project entitled "Predictive Mechanisms of Hydrogen Embrittlement" (project # 200021-149207).

References

[1] Merrick R. Mater. Performance;(United States) 1989;28.
[2] Rhodes P, Skogsberg L, Tuttle R. Corrosion 2007;63:63.
[3] Rogers H. Science 1968;159:1057.
[4] Comer JC. Choice: Current Reviews for Academic Libraries 2005;42:1053.
[5] Nagao A, Smith CD, Dadfarnia M, Sofronis P, Robertson IM. Acta Materialia 2012;60:5182.
[6] Koyama M, Akiyama E, Tsuzaki K. Corrosion Science 2012;54:1.
[7] Troiano AR. Trans. ASM 1960;52:54.
[8] Gerberich WW, Marsh P, Hoehn J, Venkateraman S, Huang H. In: Magnin T, Gras JM, editors. Proc. Int. Conf. on Corrosion-Deformation Interactions, 1993. p.633.
[9] Oriani RA, Josephic PH. Acta Metall Mater 1974;22:1065.
[10] Gerberich WW, Foeche TJ. Hydrogen enhanced decohesion in Fe-Si single crystals: implications to modelling of thresholds. In: Moody NR, editor. TMS, 1990. p.687.
[11] Oriani RA. Berichte der Bunsengesellschaft fur physikalische Chemie 1972;76:848.
[12] Gerberich WW, Marsh PG, Hoehn JW. Hydrogen Induced Cracking Mechanisms - Are There Critical Experiments? In: Moody NR, Hoehn JW, editors. Hydrogen Effects in Materials. Warrendale, PA: TMS, 1996.
[13] Birnbaum HK, Sofronis P. Mat Sci Eng a-Struct 1994;176:191.
[14] Beacham CD. Metallurgical and Materials Transactions B 1972;3:437.
[15] Robertson IM. Eng Fract Mech 2001;68:671.
[16] Westlake DG. Trans. ASM 1969;62:1000.
[17] Gahr S, Grossbeck ML, Birnbaum HK. Acta Metall Mater 1977;25:125.
[18] Shih DS, Robertson IM, Birnbaum HK. Acta Metall Mater 1988;36:111.
[19] Song J, Curtin WA. Acta Materialia 2011;59:1557.
[20] Song J, Curtin W. Nature materials 2013;12:145.
[21] Gangloff RP, Somerday BP. Gaseous Hydrogen Embrittlement of Materials in Energy Technologies: Mechanisms, modelling and future developments: Elsevier, 2012.
[22] Zmudzinski C, Blondeau R, Bretin L, Toitot M. Mem Etud Sci Rev Met 1978;75:571.
[23] Zmudzinski C, Pressouyre G, Bretin L. Commission of the European Communities (first programme on the production and utilization of hydrogen). 1982.

[24] Vehoff H, Neumann P. Acta Metall Mater 1980;28:265.
[25] Vehoff H, Klameth HK. Acta Metall Mater 1985;33:955.
[26] Vehoff H, Rothe W. Acta Metall Mater 1983;31:1781.
[27] Ferreira PJ, Robertson IM, Birnbaum HK. Acta Materialia 1999;47:2991.
[28] Ferreira PJ, Robertson IM, Birnbaum HK. Acta Materialia 1998;46:1749.
[29] Ferreira PJ, Robertson IM, Birnbaum HK. Mater Sci Forum 1996;207-:93.
[30] Teter D, Ferreira P, Robertson IM, Birnbaum HK. New Techniques for Characterizing Corrosion and Stress Corrosion 1996:53.
[31] Golovin Y. Phys Solid State+ 2008;50:2205.
[32] Katz Y, Tymiak N, Gerberich WW. Eng Fract Mech 2001;68:619.
[33] Glowacka A, Wozniak MJ, Swiatnicki WA. Rev Adv Mater Sci 2004;8:66.
[34] Gao X. Scripta Mater 2005;53:1315.
[35] Zhang L, An B, Fukuyama S, Yokogawa K. Jpn J Appl Phys 2009;48.
[36] Bahr DF, Nibur KA, Morasch KR, Field DP. Jom-J Min Met Mat S 2003;55:47.

[37] Nibur KA, Bahr DF, Somerday BP. Acta Materialia 2006;54:2677.
[38] Durst K, Backes B, Franke O, Goken M. Acta Materialia 2006;54:2547.
[39] Barnoush A, Yang B, Vehoff H. Adv Solid State Phys 2008;47:253.
[40] Barnoush A, Vehoff H. Acta Materialia 2010;58:5274.
[41] Zhang CJ, Alavi A. J Am Chem Soc 2005;127:9808.
[42] Fukai Y, Shizuku Y, Kurokawa Y. J Alloy Compd 2001;329:195.
[43] Fukai Y, SpringerLink (Online service). The Metal-Hydrogen System Basic Bulk Properties. Springer Series in Materials Science,. Berlin, Heidelberg: Springer-Verlag Berlin Heidelberg,, 2005. p.v. digital.
[44] Salehinia I, Bahr DF. Scripta Mater 2012;66:339.
[45] Personal communication.
[46] Nose S. Mol Phys 1984;52:255.
[47] Nose S. J Chem Phys 1984;81:511.
[48] Simulations using other velocities (as low as 0.1m/s) were also performed, showing similar phenomena as presented.
[49] Kelchner CL, Plimpton SJ, Hamilton JC. Phys Rev B 1998;58:11085.
[50] Honeycutt JD, Andersen HC. J Phys Chem-Us 1987;91:4950.
[51] Wen M, Li ZY. Comp Mater Sci 2012;54:28.
[52] Wen M, Zhang L, An B, Fukuyama S, Yokogawa K. Phys Rev B 2009;80.
[53] Zimmerman JA, Gao HJ, Abraham FF. Model Simul Mater Sc 2000;8:103.
[54] Plimpton S. J Comput Phys 1995;117:1.
[55] Hoover WG. Phys Rev A 1985;31:1695.
[56] Swope WC, Andersen HC, Berens PH, Wilson KR. J Chem Phys 1982;76:637.
[57] Daw MS, Baskes MI. Phys Rev B 1984;29:6443.
[58] Angelo JE, Moody NR, Baskes MI. Model Simul Mater Sc 1995;3:289.
[59] Zhou X, Zimmerman JA, Wong BM, Hoyt JJ. Journal of Materials Research 2008;23:704.
[60] Song J, Srolovitz DJ. Acta Materialia 2007;55:4759.
[61] Song J, Srolovitz DJ. Acta Materialia 2006;54:5305.
[62] Cha PR, Srolovitz DJ, Vanderlick TK. Acta Materialia 2004;52:3983.
[63] Zhu T, Li J, J. Van Vliet K, Ogata S, Yip S, Suresh S. Journal of the Mechanics and Physics of Solids 2004;52:691.
[64] Song J, Soare M, Curtin WA. Modelling and Simulation in Materials Science and Engineering 2010;18:045003.